On the Parameter Estimation and Modeling of Aggregate Power System Loads

Valery Knyazkin, *Student Member, IEEE*, Claudio Cañizares, *Senior Member, IEEE*, and Lennart Söder, *Member, IEEE*

***Abstract*— This paper addressed some theoretical and practical issues relevant to the problem of power system load modeling and identification. Two identification techniques are developed in the theoretical framework of stochastic system identification. The identification techniques presented in this paper belong to the family of output error models; both techniques are based on well-established equations describing load recovery mechanisms having a commonly recognized physical appeal. Numerical experiments with artificially created data were first performed on the proposed techniques and the estimates obtained proved to be asymptotically unbiased and achieved the corresponding Cramér-Rao lower bound. The proposed techniques were then tested using actual field measurements taken at a paper mill, and the corresponding results were used to validate a commonly used aggregate load model.**

The results reported in this paper indicate that the existing load models satisfactorily describe the actual behavior of the physical load and can be reliably estimated using the identification techniques presented herein.

***Index Terms*— Parameter estimation, power system load modeling, system identification, output error method.**

I. Introduction

ACCURATE models of power system loads are essential for analysis and simulation of the dynamic behavior of electric power systems [1]. Having accurate models of the loads that are able to reliably reflect underlying phenomena of the physical loads is important for the purposes of designing automatic control systems and optimization of their configuration. More importantly, the dynamic properties of power system loads have a major impact on system stability [1]–[3]. In particular, previous work on the subject of voltage stability reported in the literature indicates that the parameters of both static and dynamic loads have significant impact on voltage stability of the power systems [3], [4]. On the other hand, the impact of power system load models on inter-area oscillations is discussed in [1], demonstrating the influence that load parameters have on the dominant system eigenvalues. This dependence reveals the link between the effectiveness of power system damping controllers (e.g., power system stabilizers or PSS) and the correctness of the eigenstructure of the system, which is dependent on the load model.

Manuscript submitted January 2003. Revised and resubmitted June 2003. Accepted for publication July 2003.

V. Knyazkin and L. Söder are with the Department of Electrical Engineering, Royal Institute of Technology, Teknikringen 33, SE–10044, Stockholm, Sweden. (e-mail: valery@ekc.kth.se, lennart@ekc.kth.se)

C. Cañizares is with the Department of Electrical & Computer Engineering, University of Waterloo, ON, N2L-3G1, Canada (e-mail: c.canizares@ece.uwaterloo.ca)

To be able to predict the behavior of a system, reliable models of system components are needed that faithfully reflect the dynamical behavior of the actual physical components of the system. Most of the power system components can be satisfactorily modeled by considering the physical laws which govern the respective components. There are, however, some cases when power system modeling is quite a complicated exercise. Modeling power system loads is one of them. It is known that at high voltage levels, the power system loads have to be aggregated in order to obtain manageable models suitable for analysis and simulations [1]. Depending on the load type (e.g. lighting, motor load, heating, etc.), the parameters of the aggregate load model may vary in a wide range. When the parameters of all load components are well known, the parameters of the aggregate load models can be readily determined. If the parameters of separate loads are not known or the load structure is known, but the proportion of various load components is not, deriving an aggregate load becomes more difficult.

It can be argued that in the absence of precise information about a power system load, one of the most reliable ways to obtain an accurate model of the load is to apply an identification technique. That is, if field measurements of load quantities (e.g., the voltage and current/power) adequately describing its behavior are available, then a dynamic and/or static equivalent of the load can be obtained by analyzing functional relationships between these quantities.

The current paper is concerned with theoretical and numerical aspects of identification of an aggregate model of power system loads. Identification of both linear and nonlinear models of a power system load is treated. Two identification techniques are presented that belong to the so-called family of output error models. First, the estimation of the load parameters using a linear model is presented, which is followed by the presentation of a nonlinear identification technique. The statistical properties of the proposed identification methods are studied both numerically and analytically. Thus, artificially created data are analyzed numerically and the variance of the obtained estimates is compared with the corresponding Cramér-Rao lower bound. Then, in order to benchmark the identification techniques and validate the analytical load models, field measurements taken at a paper mill were used. The results obtained indicate that the load models describe the actual behavior of the load with high accuracy. Moreover, it is shown that the load model parameters can be accurately identified using the proposed techniques.

The remainder of the paper is organized as follows: Section II presents and categorizes generic load models that are presently in use; static and dynamic, linear and nonlinear models are reviewed and briefly discussed in this section. The main system-theoretic results are summarized in Section III. Aspects of system identification such as formation of the prediction error, model linearization and discretization are discussed in this section; equations for computing the Cramér-Rao lower bound of the nonlinear model are also developed in this section. Section IV presents the key results obtained by applying the main theoretical findings of this paper to two data sets. The first data set was generated artificially, while the second was obtained by collecting and processing field measurements taken at a paper mill located in Western Sweden. Finally, the main contributions of this paper are highlighted in Section V.

II. Aggregate Models of Power System Loads

In general, obtaining detailed models of power system loads is a more complicated task than modeling a particular power system component, such as, for instance, a synchronous machine. The problem is two-fold: (*a*) loads are time variant and stochastic; (*b*) in most cases, at high voltage levels the loads must be aggregated. The latter is due to the large number and types of loads connected at the transmission system level, which makes the consideration of each separate load numerically impractical and provides no insight into the system analysis. The time variance of loads can be accounted for by explicitly modeling their dynamic behavior by differential and/or difference equations.

Power system load aggregation can be performed in two ways: (*i*) analytically, by lumping similar loads and then using pre-determined values for each parameter of the load (e.g. [5] and [6]) or (*ii*) selecting a load model and then performing parameter estimation using an appropriate identification technique.

A. Static load models

Due to the importance of adequate load modeling, a large number of various static models of power system loads have been developed. Despite this diversity, in principle, they all serve one common goal: to reflect the voltage and possibly frequency dependence of the active and reactive components of the loads. For example, in [6] the following standard load models used for dynamic studies in established stability programs (e.g., EPRI's LOADSYN and ETMSP packages) are suggested:

$$P = P_0 \left[P_{a1} \left[\frac{V_L}{V_0} \right]^{K_{pv1}} [1 + K_{pf1}(f - f_0)] + (1 - P_{a1}) \left[\frac{V_L}{V_0} \right]^{K_{pv2}} \right] \quad (1)$$

$$Q = P_0 \left[Q_{a1} \left[\frac{V_L}{V_0} \right]^{K_{qv1}} [1 + K_{qf1}(f - f_0)] + [1 + K_{qf2}(f - f_0)] \left[\frac{Q_0}{P_0} - Q_{a1} \right] \left[\frac{V_L}{V_0} \right]^{K_{qv2}} \right] \quad (2)$$

where V_L and f are the load bus voltage and frequency, respectively. In equations (1)–(2), K_{pv1} and K_{pv2} represent the voltage exponents for frequency dependent and frequency independent active power load; K_{qv1} and K_{qv2} stand for the voltage exponents for the uncompensated and compensated reactive power load; K_{pf1} and K_{qf1} are the frequency sensitivity coefficients for active and uncompensated reactive power load; K_{qf2} is the frequency sensitivity coefficient for reactive compensation; and P_{a1} and Q_{a1} represent the frequency dependent fraction of active load and reactive load coefficient of uncompensated reactive load to active power load, respectively. V_0, P_0, and Q_0 denote the nominal values of the load voltage and active and reactive power of the load. It is important to note that in the models above some fraction of the load is explicitly modeled as a function of bus voltage, while the other fraction is as an explicit function of frequency.

The usefulness of a load model is directly related to the correctness of the parameters of the model. The parameters can be obtained in two ways: pre-determined values can be chosen based on the load type, or the parameters can be estimated based on field measurements. The latter is more expensive but it is preferable, since it can yield more accurate values of the load parameters.

The estimation of the parameters of a static load is relatively simple, as the load model does not involve dynamical variables; in this case, the task of parameter estimation is practically reduced to curve fitting. References [7] and [8] report successful attempts to estimate static load parameters using a modified algorithm of Broyden, Fletcher, Goldfarb, and Shanno (BFGS) and a least squares technique, respectively. It should, however, be noted that the application of any gradient-based optimization routine can potentially lead to hitting a local optimum, and thus obtaining inaccurate parameter values.

B. Dynamic load models

1) Nonlinear Dynamic Load Models: The impact that loads have on the dynamics of a power system has stimulated significant research efforts directed towards proper modeling of certain characteristics of power system loads. In many cases the use of static load models may be inappropriate due to their failure to accurately reflect the influence of the load on system stability [6], [9]; hence, since some loads do exhibit dynamical behavior (e.g., motor loads), these are represented by means of dynamical models.

It has been shown in [1] and [4] that the following models of aggregate loads can successfully capture the dominant nonlinear steady-state behavior of the load as well as load

recovery and overshoot:

$$\begin{aligned}\dot{x}(t) &= -\frac{x(t)}{T_p} + P_0\left[\frac{V_L(t)}{V_0}\right]^{N_{ps}} - P_0\left[\frac{V_L(t)}{V_0}\right]^{N_{pt}} \\ P_d(t) &= \frac{x(t)}{T_p} + P_0\left[\frac{V_L(t)}{V_0}\right]^{N_{pt}}\end{aligned} \tag{3}$$

$$\begin{aligned}\dot{z}(t) &= -\frac{z(t)}{T_q} + Q_0\left[\frac{V_L(t)}{V_0}\right]^{N_{qs}} - Q_0\left[\frac{V_L(t)}{V_0}\right]^{N_{qt}} \\ Q_d(t) &= \frac{z(t)}{T_q} + Q_0\left[\frac{V_L(t)}{V_0}\right]^{N_{qt}}\end{aligned} \tag{4}$$

In the equations above $P_d(t)$ and $Q_d(t)$ are the active and reactive power demand of the load, P_0, Q_0, and V_0 stand for the nominal active, reactive power and voltage, respectively; the parameters T_p and T_q denote the time constant of the load internal state variables $x(t)$ and $z(t)$; and the exponents N_{ps}, N_{qs}, N_{pt}, and N_{qt} are the steady state and transient voltage indices. Observe that neglecting the frequency dependence in the static load model (1)–(2), the nonlinear load model (3)–(4) is equivalent to this model in steady state, i.e., for $\dot{x}(t) = 0$.

In the remainder of the paper, the following notation will be used $\theta = [N_{ps}\ N_{pt}\ T_p^{-1}]' = [\theta_1\ \theta_2\ \theta_3]'$ and $y(t) := P_d(t)$. (Note that throughout the paper the prime denotes transposition.) In general, for a given load the exponents θ_1 and θ_2 are not known exactly; however, similarly to the case of static load models, average values for many load types have been pre-determined. For example, [1] gives the following lower and upper bounds for these indices:

$$0 \leqslant \theta_1 \leqslant 3,\ 0.5 \leqslant \theta_2 \leqslant 2.5 \tag{5}$$

For simplicity, henceforth, the voltage V_0, active and reactive power P_0, Q_0 will be assumed to be known values. Thus, the system voltage can be normalized and denoted by: $V(t) := V_L(t)/V_0$. In the subsequent sections of this paper only the model of active power (3) will be considered. The reactive power model given by (4) can be treated in exactly the same manner.

It should be noted that the load models (3)–(4) are linear in states, and the nonlinearities enter the equations as inputs and outputs. Thus, strictly speaking, the model in the identification procedure discussed in this paper should be referred to as a "Hammerstein-Wiener" model structure [10]. However, since these models are actually used in stability analysis of power systems, where load voltage magnitudes are treated as either algebraic or state variables, the model is typically referred to as a nonlinear model in this context. For this reason, and to simplify the comparisons between the two different load models discussed here, the present model is referred to as a "nonlinear" model for the remainder of the paper.

2) Linear Dynamic Load Models: When studying behavior of a system in a small proximity of a given operating point, the original nonlinear model can be approximated by a linear counterpart. That is, the nonlinear system can be linearized around an equilibrium point. Since the functions $V(t)^{\theta_1}$ and $V(t)^{\theta_2}$ are smooth for a smooth $V(t)$, the right-hand sides of (3) can be expanded in a Taylor series, resulting in the linearized model of the load [4]:

$$\begin{aligned}\Delta\dot{x}(t) &= -\theta_3\Delta x(t) + P_0\left(\theta_1 - \theta_2\right)\Delta V(t) \\ &= -A(\theta)\Delta x(t) + B(\theta)\Delta V(t) \\ \Delta y(t) &= \theta_3\Delta x(t) + P_0\theta_2\Delta V(t) \\ &= A(\theta)\Delta x(t) + D(\theta)\Delta V(t).\end{aligned} \tag{6}$$

In principle, to obtain a rough estimate of the system behavior, pre-determined values of the steady state and transient voltage indices can be used in simulations. However, as the transmission systems become more stressed, it becomes important to have more accurate estimates of the indices, since they directly influence important system characteristics such as damping (e.g., incorporation of inaccurate load characteristics in power system simulation models can lead to overestimation of system damping [9]).

As in the case of static load models, the load characteristics can be identified based on field measurements. The use of identification techniques can yield accurate estimates of load parameters, provided certain care has been exercised when selecting input signals and setting up the measurement circuits. These and related questions are treated in more detail in the next section.

III. System Identification

System identification can be defined as a collection of techniques which aim at extracting a mathematical model of a given process by analyzing relations between the input and output quantities of the process. Modern system identification has developed into a mature engineering discipline which is intensively applied in many branches of modern engineering. In this paper, only identification techniques that are relevant to the problem at hand will be reviewed; for a detailed treatment of system identification theory and practice the reader is referred to [11]–[13].

In the context of this paper, the load voltage and load power comprise the pair of input and output signals. It can be noticed that both models (3) and (4) describe the dynamic behavior of a load as functions of the nodal voltage in a noise-free environment i.e., the presence of noise is not reflected in the models. Hence, to account for the presence of noise in the measurements and since no information is available regarding the noise model, an output error model is chosen, which is known to be robust and have a plausible physical interpretation. To simplify notation, two new functions $u_1(\theta)$ and $u_2(\theta)$ are introduced:

$$\begin{aligned}u_1(\theta) &:= P_0V^{\theta_1}(t) - P_0V^{\theta_2}(t) \\ u_2(\theta) &:= P_0V^{\theta_2}(t)\end{aligned}$$

Now, the model (3) can be reformulated in a stochastic framework as:

$$\begin{aligned}\dot{x}(t) &= -\theta_3x(t) + u_1(\theta) \\ y(t) &= \theta_3x(t) + u_2(\theta) + e(t) \\ &= \hat{y}(t) + e(t).\end{aligned} \tag{7}$$

In the equation above, the term $e(t)$ represents white Gaussian noise with known statistics. Similar arguments apply to the model of reactive power.

A. Model discretization

Since measurements used in system identification are collected at predefined instants of time, the continuous-time load equations

(7) should be converted to discrete-time counterparts. In this paper, the discrete-time description of the load equations is based on the Zero-Order Hold method (ZOH) and is obtained as follows [14]:

$$x(k\ell+\ell) = F(\theta)x(k\ell) + H(\theta)u_1(k\ell) \quad (8)$$
$$y(k\ell) = \theta_3 x(k\ell) + u_2(k\ell) + e(k\ell) \quad (9)$$

where $\ell := t_{k+1} - t_k, \forall\, k \in \mathcal{I} \subseteq \mathbb{N}$, stands for the sampling interval, and the variables $F(\theta)$ and $H(\theta)$ are:

$$F(\theta) := \exp(-\theta_3 \ell), \quad (10)$$

$$\begin{aligned} H(\theta)u_1(k\ell) &= \int_{k\ell}^{k\ell+\ell} \{\exp(\theta_3(k\ell+\ell-\tau))u_1(\tau)\}\, d\tau \\ &= (1-F(\theta))\theta_3^{-1}u_1(k\ell). \end{aligned} \quad (11)$$

In equation (11), it is assumed that the input function $u_1(\tau)$ is constant and equal to $u_1(k\ell)$ for $k\ell \leqslant \tau \leqslant k\ell+\ell$.

Several numerical experiments conducted by the authors confirmed that ZOH discretization yields the least error as compared with other methods such as, for instance, the forward Euler and the trapezoidal methods. Thus, ZOH is used here to discretize the nonlinear equations (7).

B. Prediction Error for the Nonlinear Load Model

The discretized equations can be utilized as a basis for the prediction of future outputs of the dynamic system, i.e.,

$$\begin{aligned} &qx(k\ell) - F(\theta)x(k\ell) = H(\theta)u_1(k\ell) \\ &x(k\ell) = (q-F(\theta))^{-1}H(\theta)u_1(k\ell) \\ &y(k\ell|\theta) = \theta_3\left\{(q-F(\theta))^{-1}H(\theta)u_1(k\ell)\right\} + u_2(k\ell)e(k\ell) \\ &= \frac{1-F(\theta)}{q-F(\theta)}u_1(k\ell) + u_2(k\ell) + e(k\ell) \\ &= \hat{y}(k\ell|\theta) + e(k\ell). \end{aligned} \quad (12)$$

In equation (12), the symbol q denotes the forward shift operator. It is interesting to observe that the predicted value of the system output $\hat{y}(k|\theta)$ at time k equals the sum of the prefiltered input function $u_1(k)$ and input function $u_2(k)$. Finally, the prediction error is defined as the difference between the predicted and actual output of the system

$$\varepsilon(k|\theta) = y(k) - \hat{y}(k|\theta),\ \forall k \in \mathcal{I}. \quad (13)$$

C. Prediction Error for the Linear Load Model

Similarly to the nonlinear load model, let us assume that the dynamic response of the load can be satisfactorily described by a linear output error model, i.e.,

$$\Delta y(t) = A(\theta)\Delta x(t) + D(\theta)\Delta V(t) + e(t). \quad (14)$$

Applying the ZOH method to linearized load model (6), one readily obtains the discrete load model:

$$\begin{aligned} \Delta x(k\ell+\ell|\theta) &= F(\theta)\Delta x(k\ell) + \Gamma(\theta)\Delta V(k\ell) \\ \Delta y(k\ell|\theta) &= A(\theta)\Delta x(k\ell) + D(\theta)\Delta V(k\ell) + e(k\ell), \end{aligned} \quad (15)$$

where (15), $\Gamma(\theta) = H(\theta)P_0(\theta_1-\theta_2)$, where $F(\theta)$ and $H(\theta)$ are defined as in (10) and (11), respectively.

Eliminating the state variable $\Delta x(k\ell)$, the discretized output error model (15) can be rewritten in the form of a transfer function:

$$\begin{aligned} \Delta y(k\ell|\theta) &= \frac{\theta_3\Gamma(\theta)}{q-F(\theta)}\Delta V(k\ell) + e(k\ell) \\ &= P_0\frac{1-F(\theta)}{q-F(\theta)}(\theta_1-\theta_2)\Delta V(k\ell) + e(k\ell) \\ &= \Delta\hat{y}(k\ell|\theta) + e(k\ell). \end{aligned} \quad (16)$$

The prediction error for the linearized model is formulated as the difference between the measured output $\Delta y(k\ell)$ and the predicted output $\Delta\hat{y}(k\ell)$:

$$\varepsilon(k|\theta) = \Delta y(k\ell) - \Delta\hat{y}(k\ell|\theta),\ \forall k \in \mathcal{I}. \quad (17)$$

D. Minimization of the Prediction Error

Ideally, in a noise-free environment the prediction error is zero at all times, if both load model and the values of the parameter vector θ are known exactly. In practice, however, this is not achievable due to the fact that these conditions are not satisfied; moreover, field measurements always contain noise. Therefore, in the best case scenario, one can hope for keeping the prediction error reasonably small, which can be accomplished by formulating an optimization problem in which certain objective function—often a 2-norm of the prediction error vector—is minimized by varying the parameter vector θ over the feasible parameter space. We thus follow the system identification tradition and define the optimization problem as

$$\theta^* = \arg\min_{\theta\in\Omega} \frac{1}{2}\left\|\varepsilon(\theta)\right\|_2^2. \quad (18)$$

In the expression above θ^* and Ω stand for the optimal parameter vector and the feasible parameter space defined by (5), respectively.

The success of prediction error minimization depends on a number of factors, namely, (*i*) the optimization technique applied, (*ii*) the availability of a reasonable initial vector θ_0, and (*iii*) the properties of the objective function. While the first two factors in most practical cases can be relatively easy overcome, non-convexity of the objective function can in general represent a significant challenge for all gradient-based

optimization techniques. In order to avoid the traps of local minima, a robust minimization technique capable of finding the global optimum has been applied in the work reported in this paper. A brief description of this optimization method as well as the techniques used to determine the variance of the estimates are given below.

1) Adaptive Simulated Annealing: Simulated annealing (SA) can be defined as a family of general-purpose constrained optimization algorithms whose operational principles imitate the process of crystal formation in solids during gradual cooling [15], [16]. The main strength of SA algorithms lies in the fact that the SA algorithms are statistically guaranteed to find global optima of the objective function, provided the parameters of the SA are properly chosen [17].

In this paper, one of the most successful modifications of the basic SA algorithm termed *Adaptive Simulated Annealing* (ASA) is used [18]. Due to several substantial improvements, ASA performs significantly better than the basic SA algorithm and algorithms based on Cauchy annealing. The reasonable performance of ASA combined with the ability to locate global optima make its use suitable for the optimization tasks studied in this paper.

2) Cramér-Rao Lower Bound for the nonlinear load model: Determination of an optimal θ^* satisfying (18), constitutes the first step of the load identification procedure presented in this paper. The second step involves the computation of the variance of the estimates to assess the "quality" of the proposed identification procedure. The variance of the estimates depends on several factors, among which the most important for the application discussed here are the number of data samples available, the variance of noise $e(t)$, the model of the load, and the input signal.

To assess the minimum variance of the unknown parameters, the so-called Cramér-Rao Lower Bound (CRLB) is often used. By definition, CRLB is an inverse of the Fisher Information Matrix (*FIM*)

$$FIM = \mathcal{E}\left(\left(\frac{\partial \ln L(\theta,N)}{\partial\theta}\right)' \frac{\partial \ln L(\theta,N)}{\partial\theta}\right), \tag{19}$$

where N is the number of data samples available and $\mathcal{E}(\xi)$ is the expected value of ξ. The maximum likelihood function $\ln L(\theta,N)$ is defined in terms of the corresponding probability density function $L(\theta,N)$ as follows:

$$\begin{aligned} L(\theta,N) &= \frac{(2\pi)^{-N/2}}{\sqrt{\det(W)}} \exp\left[-\frac{1}{2}\left[y-\hat{y}\right]' W^{-1}\left[y-\hat{y}\right]\right] \\ &= \frac{(2\pi)^{-N/2}}{\sqrt{\det(W)}} \exp\left[-\frac{1}{2}\left\|y-\hat{y}\right\|^2_{W^{-1}}\right] \end{aligned} \tag{20}$$

In equation (20), W is a symmetric matrix representing the covariance of white Gaussian noise $e(t)$. This matrix can be used as an instrument to accentuate reliable parts of the measured data y. Often it is assumed that $W = \sigma^2 I_N$, where I_N is the identity matrix and σ^2 is the variance of $e(t)$. Without loss of generality, in the remainder of this paper it is assumed that $W \equiv I_N$, which renders the two norms $\|\cdot\|_2$ and $\|\cdot\|_{W^{-1}}$ equivalent.

The derivation of CRLB for the parameter vector θ requires computation of the gradient of the maximum likelihood function, which is equivalent to the gradient of the objective function in (18). The gradient is computed as follows: (for notational simplicity the argument θ is suppressed in the following)

$$\begin{aligned} \frac{1}{2}\frac{\partial\|\varepsilon(\theta)\|_2^2}{\partial\theta} &= \frac{1}{2}\frac{\partial\left(\varepsilon'\varepsilon\right)}{\partial\theta} \\ &= \frac{1}{2}\left[\frac{\partial\varepsilon'}{\partial\theta}\varepsilon + \left(\varepsilon'\otimes I_n\right)\frac{\partial\varepsilon}{\partial\theta}\right] \\ &= \frac{\partial\varepsilon'}{\partial\theta}\varepsilon, \end{aligned} \tag{21}$$

where the Jacobian matrix $\partial\varepsilon'/\partial\theta$ is defined by

$$\frac{\partial\varepsilon'}{\partial\theta} = \begin{bmatrix} \frac{\partial\varepsilon_1}{\partial\theta_1} & \frac{\partial\varepsilon_2}{\partial\theta_1} & \cdots & \frac{\partial\varepsilon_n}{\partial\theta_1} \\ \frac{\partial\varepsilon_1}{\partial\theta_2} & \frac{\partial\varepsilon_2}{\partial\theta_2} & \cdots & \frac{\partial\varepsilon_n}{\partial\theta_2} \\ \frac{\partial\varepsilon_1}{\partial\theta_3} & \frac{\partial\varepsilon_2}{\partial\theta_3} & \cdots & \frac{\partial\varepsilon_n}{\partial\theta_3} \end{bmatrix} \tag{22}$$

and the partial derivatives are

$$\begin{aligned} \frac{\partial\varepsilon_k}{\partial\theta_1} &= \frac{F(\theta)-1}{q-F(\theta)} P_0 V^{\theta_1}(k)\ln V(k) \\ \frac{\partial\varepsilon_k}{\partial\theta_2} &= \frac{1-q}{q-F(\theta)} P_0 V^{\theta_2}(k)\ln V(k) \\ \frac{\partial\varepsilon_k}{\partial\theta_3} &= \ell F \frac{1-q}{(q-F(\theta))^2} u_1(k). \end{aligned} \tag{23}$$

It should be noted that for the load model adopted in this paper, i.e., that given by (8)–(9), the CRLB explicitly depends on both the input signal $V(k)$ and the sampling interval ℓ. Moreover, by direct inspection of equations (22) and (23) one can immediately conclude that for $V(k) \equiv 1\ \forall k$, the matrix $\partial\varepsilon'/\partial\theta$ looses rank and as a result *FIM* becomes singular indicating that the variance of θ is infinite; that is, the parameters θ are not identifiable, when the voltage is at steady state $(V(t) = V_0)$.

It should be noted that the Jacobain (23) can be utilized to enhance the identification procedure by excluding the parameters θ_i that are weakly or non-identifiable [19], [20]. That is, one can use the algorithm proposed in [19] to determine which load parameters θ_i cannot be reliably identified using the available field data. This can be done in the following 5 steps.

1) Decompose $\partial\varepsilon_k/\partial\theta := V\Lambda V'$.
2) Inspect the eigenvalues of the Jacobian, i.e., the diagonal elements of the matrix Λ. Determine the number ρ which is equal to the number of eigenvalues of the Jacobain which are greater than some threshold value. This number indicates the number of identifiable parameters.
3) Partition $V := V_1 \oplus V_2$, where $V_1 \in \mathbb{R}^{N\times\rho}$ consists of the first ρ columns of V.
4) Factorize V_1' to obtain the orthonormal basis of the range space of V_1', the upper triangular matrix R, and the permutation matrix P, i.e., $V_1'P := QR$.

5) Use P to determine the parameters θ_i that should not be identified but rather affixed to some (approximate) values which are know beforehand.

The study reported in [19] indicates that this algorithm allows a significant reduction of the variance of the estimates of the ρ parameters even when the exact values of the affixed parameters were unknown. A more detailed description of the algorithm and its applications can be found in [19], [20]. Numerical experiments conducted in the framework of this study show that for the typical values of the load parameters the Jacobian matrix is always well-conditioned implying that all 3 parameters are identifiable; thus this algorithm is not applied in the case study discussed here.

IV. Application Examples

A. Artificial data

In order to investigate the statistical properties of the identification procedure presented in this paper, a series of experiments is conducted using artificially created data. Thus, in this section, the following issues are addressed:

- It is shown numerically that the estimates are asymptotically unbiased, which would not be the case if an unreasonable predictor is chosen.
- A rough estimate of the magnitude of bias that can be expected for the linearized model (16) is obtained, which is a basic issue in system identification that has not yet been addressed in the current literature in load modeling.
- The adequacy of the optimization routine, i.e. an adaptive simulated annealing algorithm, used in the paper is demonstrated, as the method is able to locate the global minimum of the objective function in all experiments.

The data vector $y(t_k)$ is generated with the help of a model with known parameters θ; the output $y(t_k)$ is then corrupted by Gaussian noise having known statistics, i.e., $e(t) \sim \mathcal{N}(0, \sigma^2 I)$ and the identification procedure is applied. The estimates of the parameter vector θ are analyzed in this case to assess the performance of the proposed technique.

The main goal of the numerical experiments in this section is to investigate the asymptotic behavior of the variance of the estimates $\hat{\theta}(N)$. In other words, the following relation has to be verified numerically:

$$\lim_{N\to\infty} \operatorname{var} \hat{\theta}(N) = 0 \tag{24}$$

for both linear and nonlinear load models. In expression (24) the operator var is defined as $\operatorname{var} \xi = \mathcal{E}(\xi^2)$, where ξ is a stochastic variable. To study the variance of estimates, the value of N is steadily increased and for each value of N, a series of Monte-Carlo simulations is performed. The variance is then computed and plotted versus the number of samples N. In this case study, the data are generated using the discrete-time model (8)–(9). The Monte-Carlo simulations involve 30 runs for each N, and the noise has the statistics $\mathcal{N}(0, 0.0015)$ with $\theta = [1.2\ 2.7\ 0.3448]'$. The adaptive simulated annealing optimization routine is initialized with $\theta_0 = [0.5\ 2.0\ 1.7]'$; and the feasible region Ω is given by (5), and the additional inequality $0 \leqslant \theta_3 \leqslant 10$.

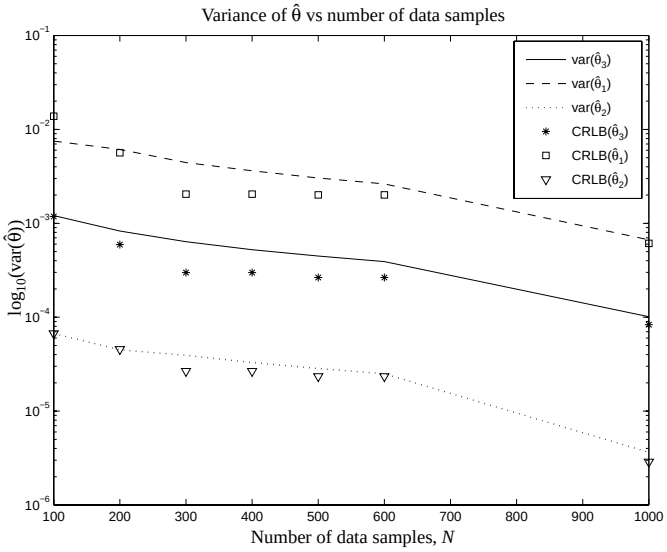

Fig. 1. Variance of the estimated parameter vector $\hat{\theta}$ versus number of samples and the corresponding Cramér-Rao Lower Bounds for the artificial data set. Nonlinear load model

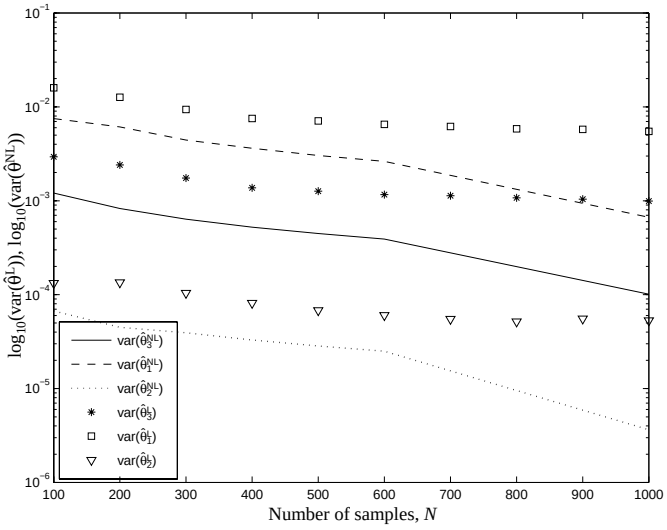

Fig. 2. Variance of the estimates of the linear and nonlinear model parameters

The results of the Monte-Carlo simulations are shown in Figures 1 and 2. Several important observations can be made regarding the performance of the nonlinear model-based identification technique:

- All three parameters θ_i are accurately estimated by applying the identification algorithm to noisy data.
- The variance of the estimates decreases as the number of samples increases. This result indicates that the estimate $\hat{\theta}$ is asymptotically unbiased, i.e., equation (24) holds. This could be expected since minimization of (18) is equivalent to maximization of the maximum likelihood function, which yields asymptotically unbiased estimates [11].
- For all N the variance of the estimates is insignificantly greater than the corresponding CRLB, implies that the proposed estimator is statistically efficient.

Comparing the results obtained with the linear and nonlinear model-based identification methods, the following can be concluded:

- The linear model-based identification method yields estimates of the parameters $\hat{\theta}^L$ acceptable for most practical purposes, since the maximum variance for this model does not exceed 2×10^{-2} for the given level of noise and number of data samples.
- The variance of $\hat{\theta}^L$ decreases as the number of data samples increases; however, in all cases, the decrease rate is not very large.
- In all cases, the variance of the estimates $\hat{\theta}^{NL}$ obtained with the nonlinear model is smaller than that obtained with the linear model. This is due to the bias induced by the use of the linearized model. In other words, for the linear model, (24) does not hold.

It should therefore be expected that the use of linear model may yield reasonable estimates of the parameters θ; however, the estimates will be biased. In general, the use of the nonlinear load model always provides more accurate estimates of the load parameters as compared to the linear model; nevertheless, the estimates obtained with the nonlinear model will also be biased, since the nonlinear model (7) is only an idealization of the actual load and thus has its limitations in terms of the accuracy of the estimates.

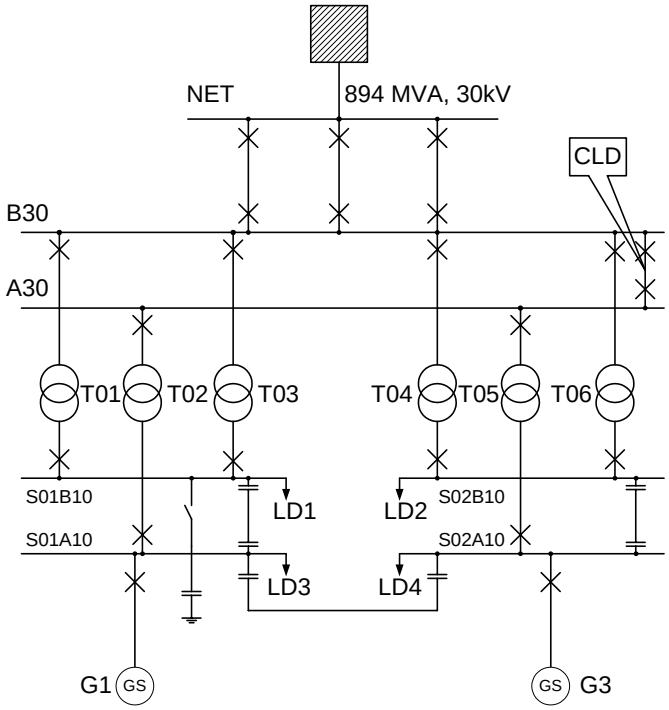

Fig. 3. Electrical diagram of the studied part of Grums paper mill

B. Application to field measurements

After verifying the adequacy of the proposed technique, it is then applied to field measurements taken at a paper mill located in the neighborhood the city of Grums, Sweden. The electrical network of the paper mill is schematically shown in Fig. 3; in this figure, only the part of the network relevant to the present case study is depicted. The network consists of two synchronous backup generators G1 and G3, four high-priority loads LD1–LD4, and six transformers T1–T6.

In normal conditions, the paper mill is fed by the grid denoted as NET. During the hours of high risk of having power supply interruptions (due to thunderstorms), the load LD1–LD4 are entirely fed by the backup generators.

In order to assure the proper and reliable operation of the paper mill, detailed dynamic simulations with accurate load models are needed; thus, a series of field measurements was obtained on May 15, 2001, in order to obtain aggregate models of LD1–LD4 and some other equipment. To the best knowledge of the authors, the load in question mainly consists of lighting, heating devices, and electrical motors. The motors are in almost all cases equipped with power converters. The load voltage was used as the input and load current as the output. Since the load models (3)–(4) use the active P_d and reactive Q_d power signals as outputs, P_d and Q_d were synthesized off-line. The sampling rate was set to 2 kHz.

An interruption of power supply to the mill may result in a substantial monetary loss. It should be noted that a step-wise voltage change could cause excessive shock to the system and trigger a power interruption. Moreover, a voltage step could result in an ill-conditioned Fisher information matrix and thus estimates with a large variance. Therefore, the backup generators were used to vary the load voltage in a smooth manner in a $\pm 3\%$ range. Extensive studies reported in [8] also suggest that the variations of voltage magnitude has little effect on the success of the parameter identification procedure, as long as the magnitude variation is a few per cent of the nominal voltage.

Given the restrictions imposed in the measuring procedure as well as the costs associated with obtaining these measurements, it was only feasible to gather one set of data at the given operating conditions. Hence, the cross-validation procedure applied here is based on a comparison between the linear (6) and nonlinear (7) load models identified using the proposed procedure and based on the same set of field measurements. Figures 4 and 5 depict the field measurements, i.e., the load voltage and active power, as well as the simulated outputs $P_d(t)$ of the linear and nonlinear models. Visual comparison of the measured and simulated power indicate that both models capture the relevant dynamics of the load; however, the nonlinear model yields better results, showing a very close match with the field measurement, as these two curves are practically indistinguishable.

Table I presents the numerical values of the parameters obtained with both linear and nonlinear system identification techniques. In the table, the error is defined as $(\hat{\theta}_i^{NL} - \hat{\theta}_i^L)/\hat{\theta}_i^{NL} \cdot 100\%$, where $\hat{\theta}_i^L$ and $\hat{\theta}_i^{NL}$, $i = 1, 2, 3$ are the estimates of the linearized and nonlinear model parameters, assuming the nonlinear model is the reference for these calculations, given the close match between this model and the actual measurements. The table reveals that the parameters identified with the linear model do not deviate significantly from those obtained with the nonlinear load identification technique. This is mainly due to the fact that the voltage

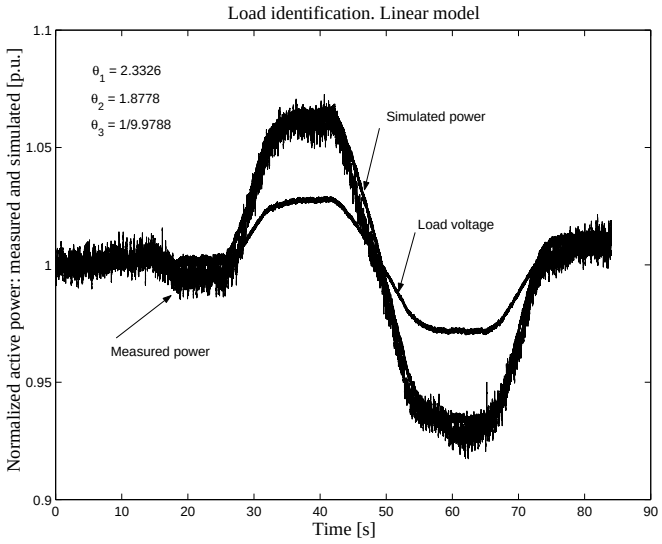

Fig. 4. Application of the proposed identification scheme to field measurements. Estimation of the parameters of active power load. Linearized model

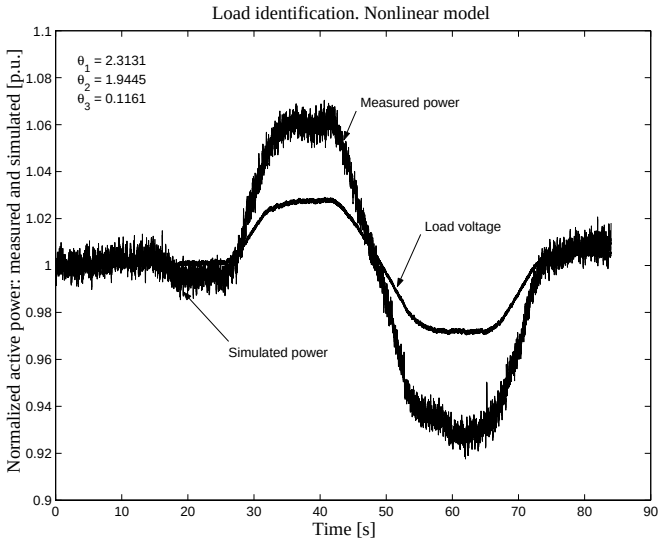

Fig. 5. Application of the proposed identification scheme to field measurements. Estimation of the parameters of active power load. Nonlinear Identification

TABLE I

COMPARISON OF THE LOAD PARAMETERS IDENTIFIED USING LINEAR AND NONLINEAR MODELS

	Linear model	Nonlinear model	Error [%]
N_{ps} [p.u.]	2.3326	2.3131	−0.8430
N_{pt} [p.u.]	1.8778	1.9445	3.4302
T_p^{-1} [s]	0.1002	0.1161	13.6951

deviation was not large and hence nonlinear effects were not very significant. However, observe that the maximum error introduced by the use of linearized model is still greater than 13%; hence, we may conclude from these results that the nonlinear model is a more accurate representation of the given aggregate load.

Notice that at different operating conditions, one would expect to obtain different values for the load parameters. However, based on the results depicted here and the fact that the load composition is not expected to change significantly for typical operating conditions, it is reasonable to expect similar trends in terms of the accuracy of the linear and nonlinear load models for representing the given aggregate load.

It is interesting to compare the values of load parameters obtained in this study with those reported in the literature. For instance, [8] cites the following value for $N_{ps} = 0.72$ for an industrial load. This value differs significantly from the one shown in Table I, which can be mainly explained by a different composition of the load. The steady state and transient voltage indices determined in [2] match those of the present paper somewhat more closely; however, the time constants T_p differ significantly, which can be explained by the absence of devices having slow dynamics, e.g., OLTC in the present case study.

V. CONCLUSIONS

Two power system load identification techniques are proposed in this paper. Well established equations describing the nonlinear recovery mechanisms of load form the basis of both techniques, which are formulated in the framework of stochastic system identification theory. Specifically, a linear and nonlinear output error estimators are introduced and analyzed, and generic equations applicable to identification of aggregate models of power system loads are developed and studied in detail.

The asymptotic behavior of the estimates is studied by means of numerical experiments with artificially created data, demonstrating that the estimates are asymptotically unbiased for the nonlinear load model and their variance attains the Cramér-Rao lower bound. To avoid numerical problems associated with possible multiple minima of the objective function, a global minimization technique was utilized. The enhanced numerical features of the minimization routine enable fast convergence to the global minimum of the objective function with a probability of 1.

The theoretical foundations presented in this paper were applied to field measurements taken at a paper mill located in the neighborhood of the city of Grums, Sweden. Both linear and nonlinear models were utilized in order to estimate the load parameters. The results show that, in principle, the linear model yields valid estimates that differ from the estimates obtained using the nonlinear model. Whenever the accuracy requirements on the numerical values of the load parameters are not stringent, linear identification can be applied for the estimation of the parameters. Alternatively, the nonlinear load modeling and identification technique presented in this paper can be used to better model the load and obtain more accurate estimates of the load parameters.

VI. Acknowledgements

The authors would like to express their gratitude to the personnel of the paper mill *Billerud AB Gruvöns Bruk* in Grums, Sweden and in particular to Mr P. Ivermark, the Manager for Electrical Maintenance of *Billerud* for his help in acquiring field data for the main case study. The help of Dr E. Thunberg of *Svenska Kraftnät* in collecting and interpreting field measurements for the case study is gratefully acknowledged.

References

[1] *Analysis and Control of Power System Oscillations*. CIGRE, Technical Report 38.01.07, December 1996.
[2] D. Karlsson and D. Hill, "Modelling and identification of nonlinear dynamic loads in power systems," *IEEE Transactions on Power Systems*, vol. 9, no. 1, pp. 157–166, February 1994.
[3] C. Taylor, *Power System Voltage Stability*, ser. Power System Engineering. McGraw-Hill, Inc., 1994.
[4] D. Hill, "Nonlinear Dynamic Load Models with Recovery for Voltage Stability Studies," *IEEE Transactions on Power Systems*, vol. 8, no. 1, pp. 166–176, February 1993.
[5] "Load representation for dynamic performance analysis (of power systems)," *IEEE Transactions on Power Systems*, vol. 8, no. 8, pp. 472–482, May 1993.
[6] "Bibliography on load models for power flow and dynamic performance simulation," *IEEE Transactions on Power Systems*, vol. 10, no. 1, pp. 523–538, February 1995.
[7] L.G.Dias and M. El-Hawary, "Nonlinear parameter estimation experiments for static load modelling in electric power systems," *IEE Proceedings on Generation, Transmission and Distribution*, vol. 136, no. 2, pp. 68–77, March 1989.
[8] W. Xu, E. Vaahedi, Y. Mansour, and J. Tamby, "Voltage stability load parameter determination from field tests on b.c. hydro's system," *IEEE Transactions on Power Systems*, vol. 12, pp. 1290–1297, August 1997.
[9] Y. Makarov, V. Maslennikov, and D. Hill, "Revealing loads having the biggest influence on power system small disturbance stability," *IEEE Transactions on Power Systems*, vol. 11, no. 4, pp. 2018–2023, November 1996.
[10] A. Garulli, L. Giarrè, and G. Zappa, "Identification of approximated models in a worst-case setting," *IEEE Transactions on Automatic Control*, vol. 47, pp. 2046–2050, December 2002.
[11] L. Ljung, *System Identification – Theory for the User*. Prentice Hall, Englewood Cliffs, N.J., 1987.
[12] ——, *System Identification Toolbox. User's Guide*. The MathWorks, Inc., 1997.
[13] O. Nelles, *Nonlinear system identification: from classical approaches to neural networks and fuzzy models*. Berlin, Springer, 2001.
[14] R. J. Vaccaro, *Digital control: a state-space approach*, ser. McGraw-Hill series in electrical and computer engineering. New York: McGraw-Hill, 1995.
[15] R. H. J. M. Otten and L. P. P. P. van Ginneken, *The Annealing Algorithm*. Kluwer Academic Publishers, 1989.
[16] Y.-H. Song and M. R. Irving, "Optimisation techniques for electrical power systems Part 2 Heuristic optimisation methods," *IEE Power Engineering Journal*, pp. 151–60, June 2001.
[17] K. Sharman, "Maximum likelihood parameter estimation by simulated annealing," *International Conference on Acoustics, Speech, and Signal Processing*, pp. 2741 –2744, April 1988.
[18] L. Ingber, "Adaptive simulated annealing (ASA): lessons learned," *Control and Cybernetics*, vol. 25, no. 1, pp. 33–54, 1996.
[19] M. Burth, G. C. Verghese, and M. Velez-Reyes, "Subset selection for improved parameter estimation in on-line identification of a synchronous generator," *IEEE Transactions on Power Systems*, vol. 14, pp. 218–225, February 1999.
[20] I. A. Hiskens, "Nonlinear dynamic model evaluation from disturbance measurements," *IEEE Transactions on Power Systems*, vol. 16, pp. 702–710, November 2001.

PLACE PHOTO HERE

Valery Knyazkin received his B.Sc. in Electrical Engineering from the Riga Technical University, Latvia in 1997 and M.Sc. and Techn. Lic. in Electrical Engineering from Royal Institute of Technology, Sweden in 1999 and 2002, respectively. He is a Ph.D. student in the Department of Electric Power Engineering, Division of Electric Power Systems at Royal Institute of Technology. He is currently working in the Department of Electrical & Computer Engineering, University of Waterloo, Canada, as a Visiting Scholar. His research interests encompass the areas of stability and control of dynamical systems, system identification, linear and nonlinear control systems.

PLACE PHOTO HERE

Claudio A. Cañizares received in April 1984 the Electrical Engineer diploma from the Escuela Politécnica Nacional (EPN), Quito-Ecuador, where he held different teaching and administrative positions from 1983 to 1993. His MS (1988) and PhD (1991) degrees in Electrical Engineering are from the University of Wisconsin-Madison. Dr. Cañizares is currently an Associate Professor and the Associate Chair for Graduate Studies at the E&CE Department of the University of Waterloo, and his research activities concentrate in the study of stability, modeling, simulation, control and computational issues in ac/dc/FACTS systems.

PLACE PHOTO HERE

Lennart Söder received his M.Sc. in Electrical Engineering and Ph.D. from the Royal Institute of Technology, Sweden in 1982 and 1988, respectively. He is currently the full professor at the Division of Electric Power Systems, Royal Institute of Technology. He also works with projects concerning deregulated electricity market and integration of wind power.